lished.
[17]B. Chu, F. J. Schoenes, and W. P. Kao, J. Amer. Chem. Soc. 90, 3042 (1968).
[18]D. Woermann and W. Sarholz, Ber. Bunsenges. Phys. Chem. 69, 319 (1965).
[19]K. Kawasaki and S. M. Lo, "Nonlocal Shear Viscosity and Order Parameter Dynamics near the Critical Point of Fluid" (to be published).

Superfluid Helium in Restricted Geometries*

Timothy C. Padmore
Laboratory of Atomic and Solid State Physics, Cornell University, Ithaca, New York 14850
(Received 29 February 1972)

Superfluid flow in restricted geometries is discussed in the framework of the Landau quasiparticle theory. A recently observed linear temperature dependence of ρ_n for helium flowing in powders is explained in terms of a model geometry which can be fairly described as "zero-dimensional." Further experiments are suggested for exploring other features of restricted geometries and testing the zero-dimensional model.

Measurements of superfluid helium flow in compressed powders and Vycor glass were reported recently by Pobell *et al.*[1] They found that the normal fluid density ρ_n was much enhanced over its bulk value. In addition, a striking linear dependence of ρ_n on temperature was observed for $T \lesssim 0.5$ K. The fact that the experiments were performed in the temperature range $0.1\ \text{K} \lesssim T \lesssim 1$ K allows one to take advantage of the Landau quasiparticle picture[2] to discuss the experiments theoretically. In this paper are advanced some very simple arguments, based on the quasiparticle picture, which allow us to understand this result. In addition, specific predictions are given for ρ_n and the specific heat in various (experimentally realizable) geometries.

Consider first two simple examples of restricted dimensionality: flow between parallel plates, and flow in a straight tube of rectangular cross section. These geometries and the coordinate system for the problem are illustrated in Figs. 1(a) and 1(b). (Ignore, for the time being, the dashed lines and the dimension d_0.)

The pore sizes in the experiments are generally ~20–100 Å. We will therefore assume that the dimensions (d_2, d_1) in the examples are much greater than either the superfluid healing length (~1 Å), the range of the wall potential (~2–3 Å), or the roton wavelength (~4 Å). Consequently, we do not expect any important contributions to the thermodynamics from the surfaces *per se* (for example, via localized surface states), and we can apply the Landau treatment[2] to calculate ρ_n. We also expect that for $T \lesssim 0.5$ K the roton contributions can, as usual, be ignored and will therefore consider only phonon states assuming the usual dispersion relation $\epsilon_0(k) = \hbar c k$, where c is the sound velocity and k the phonon wave number.

Suppose that the background fluid has a velocity $\vec{v}_s = v_s \hat{z}$. Then the momentum density is

$$\vec{j} = \rho \vec{v}_s + V^{-1} \sum_{\vec{k}} \hbar \vec{k} n_{\vec{k}}, \tag{1}$$

where in the second term (which gives the momentum of the excitations) $n_{\vec{k}}$ denotes the number of states with wave number $\vec{k}$ and V is the volume. It is elementary to show that $n_{\vec{k}} = n(\epsilon(\vec{k}))$, where $n(\epsilon) = [\exp(\epsilon/k_B T) - 1]^{-1}$ and $\epsilon(\vec{k})$, the spectrum in the frame of the walls, equals $\epsilon_0(\vec{k}) + \hbar \vec{k} \cdot \vec{v}_s$. Provided $v_s \ll c$, Eq. (1) can be linearized to give

$$\begin{aligned} \vec{j} &\approx \rho \vec{v}_s + \hbar^2 V^{-1} \sum_{\vec{k}} (\vec{v}_s \cdot \vec{k}) \vec{k}\, dn(\epsilon_0)/d\epsilon \\ &\equiv (\rho - \rho_n) \vec{v}_s , \end{aligned} \tag{2}$$

which defines

$$\rho_n = -\hbar^2 V^{-1} \sum_{\vec{k}} k_z^2\, dn(\epsilon_0)/d\epsilon . \tag{3}$$

In the bulk system the $\vec{k}$ sum is $V(2\pi)^{-3} \int d^3k$. For the flow between the plates it becomes $A(2\pi)^{-2} \times \sum_{k_x} \int dk_y dk_z$, where A is the area of the plates.

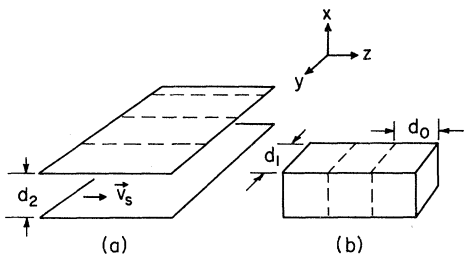

FIG. 1. Geometries for 2D and 1D superfluid flow. Dashed lines, positions of the repulsive potentials in the Kronig-Penney construction.

The k_x sum is over values $k_x = m\pi d_2^{-1}, m = 0,1,2,\cdots$. The system will be considered "two-dimensional" (2D) if the energy $\hbar c\pi d_2^{-1} \gg k_B T$. (For $d_2 = 100$ Å, this energy corresponds to about 0.5 K.) In that case only the $k_x = 0$ modes will be excited so the discrete sum reduces to a single term and the sum over $\vec{k}$ becomes $A(2\pi)^{-2}\int dk_y dk_z$. A similar argument for the tube [Fig. 1(b)] yields the 1D result $\sum_{\vec{k}} \to L(2\pi)^{-1}\int dk_z$, where L is the length of the tube. The integrations are elementary. Denoting by $\rho_n^{(3)}$, $\rho_n^{(2)}$, and $\rho_n^{(1)}$ the normal density in the bulk, 2D, and 1D systems, respectively, one has

$$\rho_n^{(3)} = (2\pi^2/45)\hbar c^{-1}\lambda^{-4}, \tag{4a}$$

$$\rho_n^{(2)} = [\tfrac{3}{2}\zeta(3)/\pi]\hbar c^{-1}\lambda^{-3}d_2^{-1}, \tag{4b}$$

$$\rho_n^{(1)} = (\tfrac{1}{3}\pi)\hbar c^{-1}\lambda^{-2}(d_2 d_1)^{-1}, \tag{4c}$$

provided that

$$\hbar c\pi d_i^{-1} \gg k_B T, \quad i = 1, 2. \tag{5}$$

The parameter $\lambda = \hbar c(k_B T)^{-1}$ may be thought of as the wavelength of a typical thermal phonon. Aside from numerical factors one has $\rho_n^{(2)} \sim (\lambda/d_2)\rho_n^{(3)}$ and $\rho_n^{(1)} \sim (\lambda/d_1)\rho_n^{(2)}$. Since $\lambda \gg d_i$, ρ_n is larger the smaller the dimension of the system. Also note that $\rho_n^{(N)} \sim T^{N+1}$.

Corrections to Eqs. (4), if (5) is imperfectly satisfied, are small—on the order of $\exp(-\lambda/d_i)$. In the opposite limits ($\lambda \ll d_1$ and/or d_2) one recovers the result for a higher dimensionality. In case this latter limit is not well satisfied, however, the corrections are nontrivial. (The error comes from approximating a sum by an integral.) Denoting by $\rho_n^{(3^-)}$ the result for the plate geometry with d_2 large and by $\rho_n^{(2^-)}$ the result for the tube geometry if d_1 is large (and d_2 small), one has, to first order in λ/d_i,

$$\rho_n^{(3^-)} \approx \rho_n^{(3)}\left[1 + \frac{135\zeta(3)}{8\pi^3}\frac{\lambda}{d_2}\right], \tag{6a}$$

$$\rho_n^{(2^-)} \approx \rho_n^{(2)}\left[1 + \frac{\pi^2}{9\zeta(3)}\frac{\lambda}{d_1}\right]. \tag{6b}$$

Normally one thinks of the density of states (number per unit volume) in a given energy range as being independent of V. This is not true, of course, if the energy range is too small. If (5) holds for, say, $i = 2$, then the low-energy ($\sim k_B T$) states all have $k_x = 0$, and their number is independent of d_2; therefore the density of states goes like d_2^{-1}. This increased density of low-energy states is the reason for the enhanced ρ_n in the confining geometry.

It is interesting, and important to an understanding of the "zero-dimensional" case, to look a little more closely at how this extra density of states arises. Consider the following construction for passing from the 2D to the 1D result without changing the volume of the system. Imagine subdividing the volume between the plates with a periodic repulsive potential

$$U(x) = U_0 \sum_{l=-\infty}^{\infty} \delta(y - l d_1)$$

[indicated by dashed lines in Fig. 1(a)]. Then by turning on U_0 adiabatically we can keep track of all the states, and see in detail where the extra low-energy states come from. This potential is familiar in solid-state physics as the Kronig-Penney model[3] for electron bands. There the repulsive potential induces dimples in the electron wave function, and this pushes up the energy of the small-k modes. For large U_0 the dimples become nodes, practically, and the bands become very flat with large band gaps (see inset in Fig. 2).

Almost exactly the same thing happens in the phonon system, the important difference being that there is no "localization energy" for the collective excitation. By this I mean that the zero-wave-number or quiescent mode always has zero energy relative to the background, regardless of the arrangement of external potentials. What happens then as U_0 is turned on is that (relative to the ground-state energy) the energy of states with $k_y > 0$ falls and the band again becomes flat. When $U_0 \to \infty$, states with given k_z and $0 \leq |k_y| \leq \pi d_1^{-1}$ become degenerate; the degeneracy is the factor

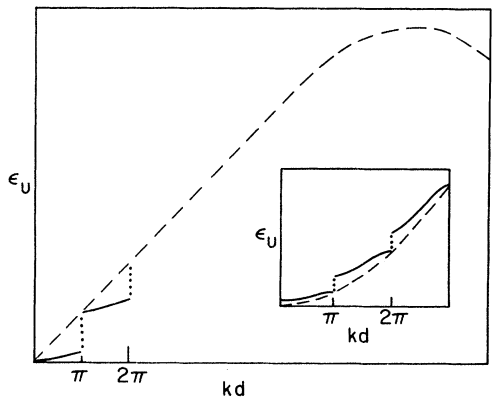

FIG. 2. Sketch of phonon dispersion relation expected for a moderately large U_0. The average slope of the section for $0 \leq kd \leq \pi$ is, roughly, $\hbar c'$. Dashed line, particle spectrum in helium. Inset, corresponding spectrum for a particle in a Kronig-Penney potential (Ref. 3).

by which the density of states increases in the transition to 1D. The "wave-function" argument is a little different this time—what happens now is that near the potential surfaces one can have relatively large ($\sim\pi$) phase changes in the wave function associated with the excitation. This allows the phase variation associated with a relatively large-k_y mode ($k_y \sim \pi d_1^{-1}$) to be taken up at the interfaces and the wave function can be rather flat elsewhere. The ground-state energy already includes a contribution equal to the energy associated with the curvature near the surface, so the relative excitation energy goes to zero ($|k_y| \leq \pi d_1^{-1}$) as $U_0 \to \infty$.[4] The qualitative behavior of the spectrum for $k_z = 0$ and finite U_0 is sketched in Fig. 2, where kd stands for $k_y d_1$ and $k_z = 0$.

Let us now consider the interesting problem of flow through a powder.[5] The detailed structure of the open space is unknown, but one can say at least that it is some complicated, irregular network of holes and cracks, with dimensions $\lesssim 100$ Å. Equations (4) and the subsequent discussion demonstrate the importance of the number of "long" (big compared to λ) dimensions of the geometry. The salient feature of the powder geometry is that there is *no* long dimension, the helium being constrained significantly, and equally, in all three dimensions.

It is possible, moreover, to think of a model which incorporates just the feature of "zero dimensionality," but which is otherwise sufficiently regular that one can draw some intelligent conclusions. Thus, imagine the 1D channel of Fig. 1(b) with a periodic potential (indicated by dashed lines)

$$U(z) = U_0 \sum_{l=-\infty}^{\infty} \delta(z - l d_0),$$

where $d_0 \sim d_1 \sim d_2 \ll \lambda$. Since condition (5) is satisfied $\sum_{\vec{k}}$ becomes $(2\pi)^{-1} L \int dk_z$ as for the 1D case, and we have only to consider the k_z dependence of the spectrum. Going through the same arguments as before, we conclude that the spectrum, in the absence of flow, has the qualitative form

$$\begin{aligned} &\epsilon_U(k_z) \approx \hbar c' k_z, \quad |k_z| \leq \pi d_0^{-1}, \\ &\epsilon_U(k_z) \gtrsim \hbar c \pi d_0^{-1}, \quad |k_z| > \pi d_0^{-1}, \end{aligned} \tag{7}$$

where $c' < c$. (Figure 2 represents the form of this spectrum if now kd is identified as $k_z d_0$.) One cannot, however, immediately substitute ϵ_U for ϵ_0 in Eq. (3) for ρ_n. Since, even in the model system, v_s varies locally, the relation $\epsilon(k_z) = \epsilon_U(k_z) + \hbar k_z v_s$, required to derive (3), must be modified. Denote by $\bar{v}_s$ the average superfluid velocity (equal nearly everywhere, if the healing length is small, to the local velocity). To first order in $\bar{v}_s$, i.e., $\bar{v}_s \ll c, c'$, we expect

$$\epsilon(k_z) \approx \epsilon_U(k_z) + \beta(k_z) \hbar k_z \bar{v}_s, \tag{8}$$

which introduces the dimensionless expansion coefficient β as a factor after $\sum_{\vec{k}}$ in (3). If $U_0 = 0$, β equals 1, and the equality is exact. Now β can only depend on k_z via dimensionless combinations $k_z \times$ length. The relevant lengths in the problem are d_0, the superfluid healing length, and a length derived from the potential strength. Only $k_z d_0$ is of order unity in the range $0 \leq |k_z| \leq \pi d_0^{-1}$. To leading order in the other dimensionless constants one expects $\beta = \beta(k_z d_0)$. We can now proceed to calculate ρ_n as in the 1D case. Put $T_0 = \hbar c d_0^{-1} k_B^{-1}$, $T_0' = \hbar c' \pi d_0^{-1} k_B^{-1}$. Then, provided we satisfy

$$T_0' \ll T \ll T_0 \tag{9}$$

(which implies $c' \ll c$), the normal density is

$$\rho_n^{(0)} = B \hbar c'^{-1} \lambda'^{-1} (d_2 d_1 d_0)^{-1}, \tag{4d}$$

where $B = (2\pi)^{-1} \int_{-\pi}^{\pi} \beta(x)\, dx$, and $\lambda' = \hbar c' (k_B T)^{-1}$. Note the linear T dependence.

The second inequality in (9) is the same as (5) and guarantees that only $|k_z| \leq \pi d_0^{-1}$ contributes to $\rho_n^{(0)}$; the first inequality allows an expansion of the exponentials in the integral. Because of (7) the 0D case is qualitatively different from 1D, 2D, or 3D; in particular note that $\rho_n^{(0)} \to \infty$ for $c' \to 0$.[6] Furthermore, for $T \to 0$ the answer reverts to the 1D result,[7] except that c is replaced by c' in Eq. (4c).

Of course the model is hardly a realistic representation of the real powder. For the mechanism just described to account for the linear T dependence, however, one requires only that (as in the model) there be few momentum-carrying states with energies $\sim k_B T$, and that there be a large density of such states for lower energies. The reasonable assumption that the powder geometry comprises open volumes, fairly uniform in size, and connected by substantially smaller cracks or channels is probably sufficient[8] to satisfy the above requirement.

In addition we must check that the numbers are roughly correct. Suppose, for simplicity, $d_2 = d_1 = d_0 =$ the "pore size" from Pobell *et al.*,[1] and take $B = 1$. (In any case B can be absorbed into the free parameter c'.) Then comparing (4d) with the linear part[9] of their experimental curves, one finds the results summarized in Table I. There are several different consistency checks.

TABLE I. Parameters for the powder geometry.

Pore size (Å)	c/c'	T_0' (K)	T_0 (K)
10–15	20–35	0.3–0.1	5–4
20–40	30–90	0.09–0.015	3–1
~50	~40	~0.03	1

In particular, Eq. (9) should be satisfied in the range where ρ_n is linear, and c/c' should be fairly large. Since it is not obvious that c/c' should vary in a particular way as the powder is compressed, it is not surprising that a constant value, $c/c' \sim 35$, is consistent with all three experiments. This value is a little large to be easily justified,[8] but the result is acceptable given our coarse estimate of the other four factors in (4d). The predicted value of T_0' is an indication of the temperature at which one might expect to see ρ_n begin to revert to T^2 dependence.[7] It appears that, for the smaller pores, such temperatures may be quite accessible.

Careful measurements of ρ_n in a regular geometry, where the d_i would necessarily be larger, would also be interesting since Eqs. (6) predict that there will be observable effects even if d_i is rather larger than λ. A further class of experiments would be to measure specific heats in restricted geometries. One has, in the limits defined above,

$$C_V^{(3)} = (2\pi^2/15)k_B\lambda^{-3}, \tag{10a}$$

$$C_V^{(2)} = [3\zeta(3)/\pi]k_B\lambda^{-2}d_2^{-1}, \tag{10b}$$

$$C_V^{(1)} = (\tfrac{1}{3}\pi)k_B\lambda^{-1}(d_2d_1)^{-1}, \tag{10c}$$

$$C_V^{(0)} = k_B(d_2d_1d_0)^{-1}. \tag{10d}$$

Note that (10d) reverts to $C_V \sim T$ for $T \to 0$ (as required by Nernst's law).[10] Equation (10d) is just the statement that the system consists of weakly coupled units, of volume $d_2d_1d_0$, and with no accessible internal degrees of freedom. Note that the specific heat results do not involve the parameter c' or the function β. C_V measurements would therefore constitute an even more direct test of the central thesis of this paper, namely, the importance of dimensionality as here defined.

I would like to thank Michael Fisher, John Reppy, Josef Sak, and John Wilkins for useful discussions.

*Work supported by the National Science Foundation through Grant No. GP-27355.

[1]F. D. M. Pobell, H. W. Chan, L. R. Corruccini, R. P. Henkel, S. W. Schwenterly, and J. D. Reppy, Phys. Rev. Lett. 28, 542 (1972).

[2]L. Landau, J. Phys. (U.S.S.R.) 5, 71 (1941).

[3]R. de L. Kronig and W. G. Penney, Proc. Roy. Soc., Ser. A 130, 499 (1930).

[4]These heuristic arguments are supported by calculations on a model superfluid system, namely, the weakly interacting Bose gas. These calculations will be published elsewhere.

[5]The material used in the experiments which shows the linear T dependence is compressed lampblack. The lampblack particles are fairly uniform spherules about 100 Å in diameter.

[6]This is to be expected since $c' \to 0$ corresponds to the cells becoming totally isolated. The correct answer is $\rho_n^{(0)} \to \rho$; the theory, which is consistent only if $\rho_n/\rho \ll 1$, does the best it can with $\rho_n^{(0)} \to \infty$.

[7]The $T \to 0$ behavior is not necessarily $\sim T^2$ as implied by the model. We could reasonably (considering the presumed isotropy of the powder) have substituted δ-function potentials for *all* the cell boundaries. Given (8), (4d) still would hold, but for $T \to 0$ we would recover a T^4 law. I feel the criterion for deciding which model is appropriate is the degree of connectivity of the powder.

[8]Classical sound waves with wavelength $\gtrsim A^{1/2}$ propagate in such a geometry with a velocity $c' \sim (a/A)^{1/2}c$, where a and A are, respectively, the smallest and largest cross sections.

[9]Contributing to the nonlinearities at higher temperature are failure (for large pores) to satisfy $T \ll T_0$, proximity to the phase transition at T_λ, and the contribution of rotons. The last could be more important for very small pores since the roton gap may be modified due to failure of the condition, roton size $\ll$ pore size.

[10]Or T^2, or T^3. See Ref. 1.